Electrical and emission characteristics of a C-to-C N_2 laser

J. DE LA ROSA AND A. VÁZQUEZ-MARTÍNEZ
Sección de Estudios de Posgrado e Investigación
Escuela Superior de Ingeniería Mecánica y Eléctrica
Instituto Politécnico Nacional
Recibido el 4 de mayo de 1994; aceptado el 6 de julio de 1994

ABSTRACT. The electrical and optical characteristics of a C-to-C N_2 laser are experimentally investigated. Current and voltage appearing in different points of the circuit are reported. From these measurements one can study the behavior of the circuit, which has not been completely described up to date. The natural frequencies and the damping constant of the laser discharge circuit were calculated from the current and voltage waveforms. The laser used in the experiments provides pulses with energies of about 40 μJ and efficiencies in the range from 0.15×10^{-4} to 0.35×10^{-4}.

RESUMEN. Se han investigado experimentalmente las características ópticas y eléctricas de un láser de N_2 basado en un circuito de transferencia de carga. Se reportan las corrientes y voltajes que aparecen en diferentes puntos del sistema. A partir de estas mediciones uno puede estudiar el comportamiento del circuito que hasta ahora no ha sido explicado completamente. Se calculó la resistencia e inductancia equivalente de la descarga láser a partir de las formas de onda de corriente y voltaje. El láser empleado en los experimentos proporciona pulsos con energías de aproximadamente 40 μJ y eficiencias en el intervalo de 0.15×10^{-4} a 0.35×10^{-4}.

PACS: 42.55

1. INTRODUCTION

Fast high voltage pulsed discharges are currently used to excite high power N_2 gas lasers. The main problem in the construction of N_2 lasers is how to put an amount of sufficiently high energy into the laser medium in the proper time. Some excitations circuits have been proposed, and the charge transfer (C-to-C) circuit is widely used for this purpose. As it can be seen in Fig. 1, the circuit is composed of a spark gap (SG) as a fast switch, the laser head and two capacitors, one of them parallel connected to the laser head. When high voltage is applied, only C_c is initially charged until the breakdown voltage V_{co} is reached across the SG. At this potential, the SG fires and C_c begins to discharge charging C_p and overvolting the laser gap until breakdown takes place; then, C_c and C_p discharge trough the laser head.

In recent years there has been some research in order to study the electrical behavior of this circuit. Papadopoulus and Serafetinides [1] have obtained some theoretical results which are not so obvious when compared to experimental ones. The main problem is that until now accurate voltage waveforms have been reported but not current measurements. In this work, we report voltage, current and emission measurements carried out on a

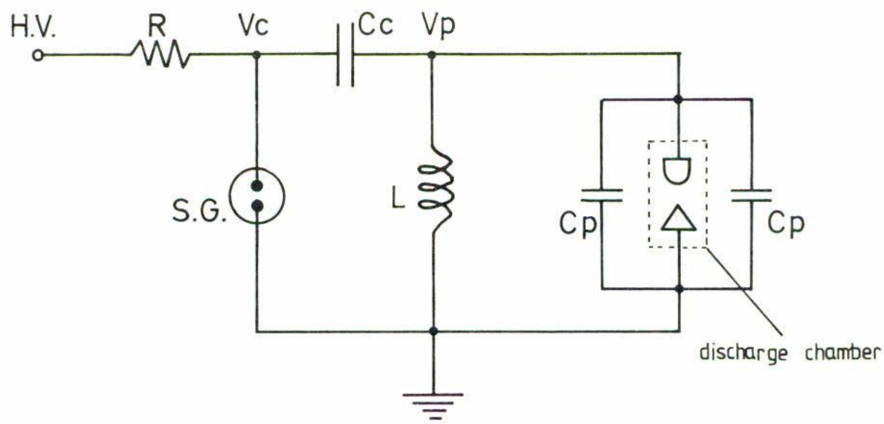

FIGURE 1. Schematic diagram of the charge transfer circuit.

N_2 laser based in such configuration. The current waveforms were obtained through a longitudinal magnetic coil developed in our laboratory [2].

2. EXPERIMENTAL SETUP

Figure 2 shows the mechanical construction of the laser. The gas envelope of the laser is a teflon structure in which the electrodes are inserted and fixed. The inductance of the connection between the laser head and the discharge capacitor is minimized by screwing this capacitor directly on to the copper plates supporting the electrodes. The upper electrode exhibits a cylindrical profile and the lower one is sharp. Both were rounded at the ends to avoid the generation of spark channels. The overall length of the discharge was 22.5 cm and the interelectrode spacing was 7 mm. The discharge capacitor, C_p, consisted of two flat capacitors made of commercial double sided copper circuit board. The charge capacitor was made of aluminum foil and polyethylene as a dielectric, rolled on a cylindrical piece of PVC. The charge capacitor and the spark gap were directly mounted on to the supporting plate of the upper electrode. The upper electrode of the spark gap is connected to the grounded sheet of both discharge capacitors. The breakdown voltage V_{co} of the spark gap is controlled by changing its interelectrode separation. High grade purity N_2 filled the discharge chamber. The optical resonator is composed of a totally reflective mirror and a transparent quartz window.

The voltages were measured with two equal high voltage probes, Tektronix P6015. The current I_{laser} was measured with an axial auto-integrating coil developed in our laboratory. The laser output energy was measured using a pyroelectric detector (Laser Precision Co. RPJ735) connected to an energy meter (Laser precision Co.RJ7610.) The optical pulses were monitored through a fast photodiode (Motorola MRD721.)

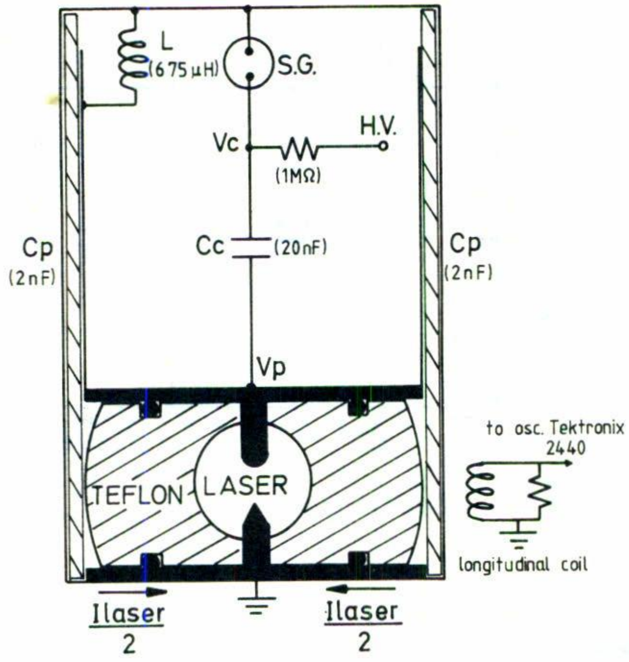

FIGURE 2. Cross sectional view of the laser used in the experiments.

3. ELECTRICAL BEHAVIOR

To analyze the behavior of the system, each discharge taking place in the circuit is simulated by an inductance and a resistance connected in series (see Fig. 3.) L_{sg} and R_{sg} stand for the inductance and resistance associated to the spark gap loop respectively, and L_{laser} and R_{laser} stand for the analogous parameters of the laser loop. Figure 4 shows the observed voltage and current waveforms appearing in the circuit. The process initiates with the triggering of the spark gap at the instant t_0, the capacitor C_c transfers energy to the discharge one up to the instant t_1 when the laser discharge initiates.

From Fig. 4 one can see that after the SG triggers the voltage V_c goes on decreasing while the voltage V_p in C_p increases (negatively) until break down occurs in the laser head; at this instant the current across the laser, I_{laser} begins to increase very rapidly; the optical pulse appears at the peak of this current pulse.

In Fig. 5 we observe the process at a larger temporal scale. All the waveforms show the superposition of two signals with different frequencies. One of them is a fast oscillation (clearly seen in V_c and V_p, and in the first 200 ns in I_{laser}) with an average period $T_1 =$ 60 ns. The other one is a slower envelope with an average period $T_2 = 204$ ns.

The differential equation governing the performance of the entire circuit after t_0 is given by the relation [3]

$$\frac{d^4I}{dt^4} + K\frac{d^3I}{dt^3} + L\frac{d^2I}{dt^2} + M\frac{dI}{dt} + NI = 0, \tag{1}$$

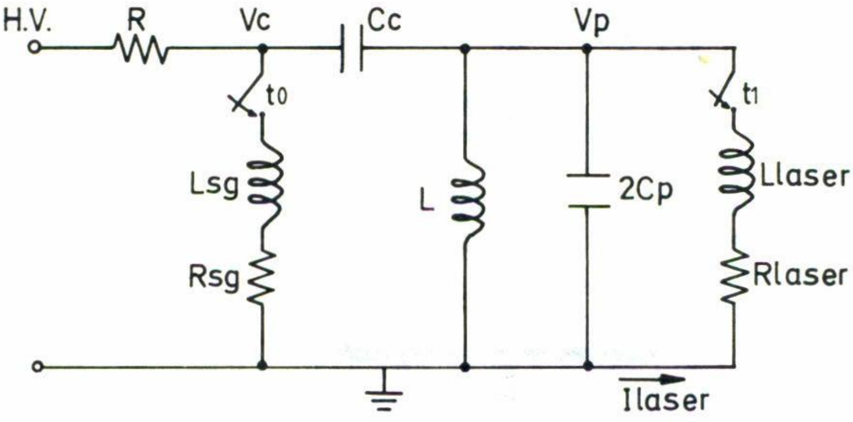

FIGURE 3. Equivalent circuit for the C-to-C circuit.

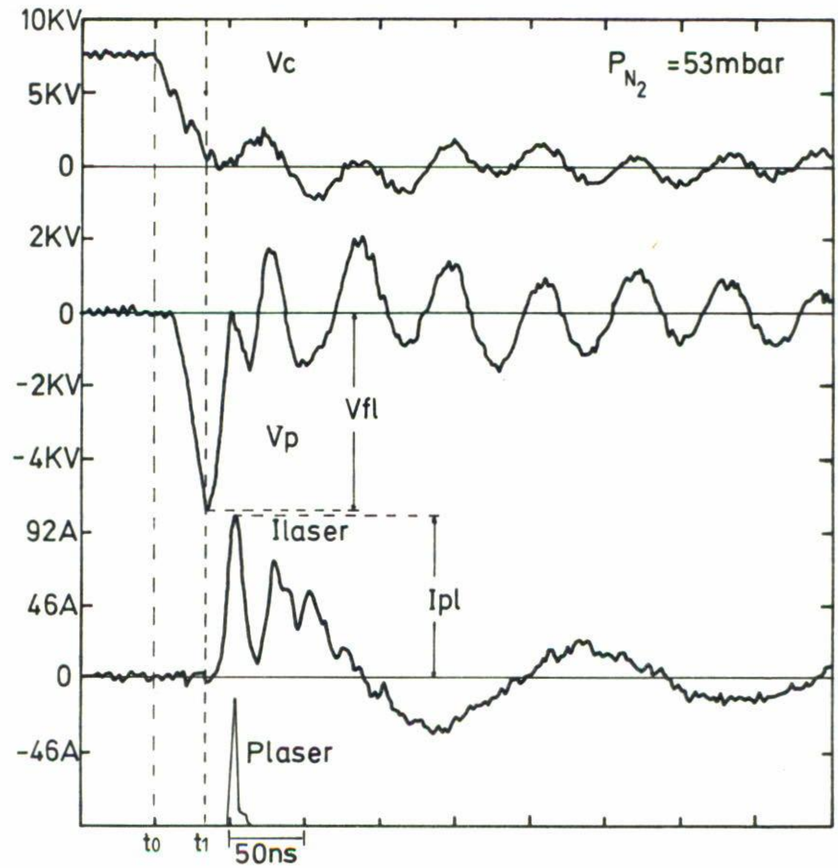

FIGURE 4. Waveforms appearing when the laser operates. From top to bottom: 1) Voltage in point V_c of Fig. 3; 2) voltage in point V_p of Fig. 3; 3) current across the laser gap; 4) laser pulse. Horizontal scale: 50 ns/div.

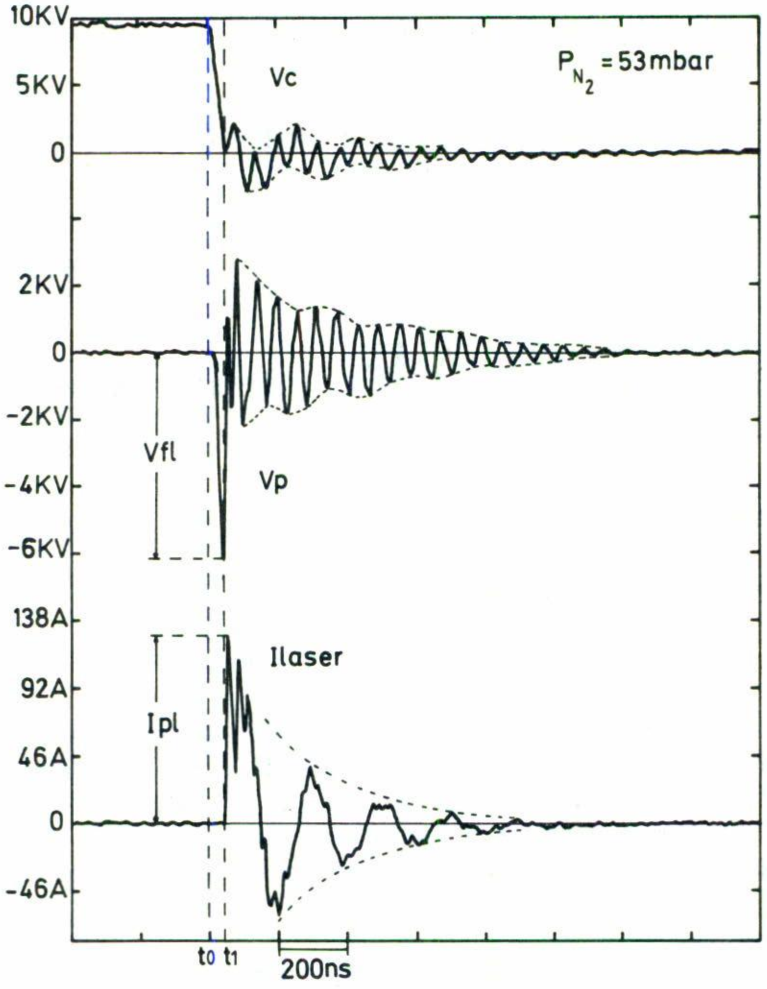

FIGURE 5. Evolution of voltages and current at a larger temporal scale. Horizontal scale: 200 ns/div.

where $I = I_1$ $(i = 1, 2, 3)$ in Fig. 3. The same equation is valid for V_p and V_c, and

$$K = \frac{R_{\text{sg}}}{L_{\text{sg}}} + \frac{R_{\text{laser}}}{L_{\text{laser}}},$$

$$L = \frac{1}{L_{\text{sg}} C_c} + \frac{1}{L_{\text{laser}} C_c} + \frac{1}{L_{\text{laser}} 2C_p} + \frac{R_{\text{sg}}}{L_{\text{sg}}} \frac{R_{\text{laser}}}{L_{\text{laser}}},$$

$$M = \frac{R_{\text{sg}}}{L_{\text{sg}}} \frac{1}{2C_p L_{\text{laser}}} + \frac{R_{\text{sg}}}{L_{\text{sg}}} \frac{1}{L_{\text{laser}} C_c} + \frac{R_{\text{laser}}}{L_{\text{laser}}} \frac{1}{L_{\text{sg}} C_c},$$

$$N = \frac{1}{2C_p C_c L_{\text{sg}} L_{\text{laser}}}.$$

The solution of Eq. (1) when $R_{\rm sg}$, $L_{\rm sg}$, $R_{\rm laser}$, and $L_{\rm laser}$ are considered to be constants is obtained in Ref. [3]:

$$I(t) = A\exp[-\alpha_1 t]\cos(\omega_1 t + \phi_1) + B\exp[-\alpha_2 t]\cos(\omega_2 t + \phi_2), \tag{2}$$

where

$$\omega_1^2 = -\frac{C_k}{2} + \frac{\sqrt{C_B}}{2} - \frac{K}{4}\frac{\sqrt{C_A}}{2}, \qquad \alpha_1 = \tfrac{1}{4}\left(K + \sqrt{C_A}\right),$$

$$\omega_2^2 = -\frac{C_k}{2} - \frac{\sqrt{C_B}}{2} + \frac{K}{4}\frac{\sqrt{C_A}}{2}, \qquad \alpha_1 = \tfrac{1}{4}\left(K - \sqrt{C_A}\right),$$

and

$$C_A = K^2 - 4L + 4\varphi_r, \qquad C_B = \varphi_r^2 - 4N, \qquad C_k = K^2/4 - L/2 - \varphi_r/2;$$

φ_r is a real root of the cubic equation

$$\varphi^3 - L\varphi^2 - (KM - 4N)\varphi + (4LN - M^2 - K^2N) = 0.$$

Since the two signals of different frequencies are clearly distinguished from the current waveforms, it is easy to determine the parameters of Eq. (2). According to Fig. 5, for the slower oscillation (frequency ω_2) appearing in $I_{\rm laser}$ the estimated damped parameter $\alpha_2 = 4.3 \times 10^6\ {\rm s}^{-1}$. For the faster oscillation (frequency ω_1) $\alpha_1 = 70 \times 10^6\ {\rm s}^{-1}$.

Thus, the current and voltage waveforms shown in Fig. 5 are approximately described by

$$I = I_1\exp[-\alpha_1 t]\sin(\omega_1 t) + I_2\exp[-\alpha_2 t]\sin(\omega_2 t),$$

$$V_c = V_{c1}\exp[-\alpha_1 t]\sin(\omega_1 t) + V_{c2}\exp[-\alpha_2 t]\sin(\omega_2 t + \pi/2).$$

In the case of V_p its equation is not so obvious because in the very beginning of the laser discharge, the time dependence of V_p shows some non-linear behavior that could be attributed to the time dependence of $R_{\rm laser}$, $L_{\rm laser}$, $R_{\rm sg}$, $L_{\rm sg}$.

Figure 6 shows the laser firing voltage $V_{\rm f1}$ and the peak current $I_{\rm p1}$ in the laser chamber as a function of the charging voltage $V_{\rm c0}$ for a constant pressure (53 mbar). Both voltage and current increase with the charging voltage and consequently the laser output energy also does; Fig. 7 shows this dependence of the laser energy $E_{\rm laser}$ on the charging voltage; the dependence of the laser efficiency η on the same parameter is also shown.

The dependence of the firing voltage on the charging voltage is explained if we consider the time required for the discharge to develop. From Fig. 8 one can see that the risetime in the first cycle of voltage V_p, t_r, decreases with the charging voltage, and Fig. 9 shows that the laser firing voltage reaches higher values for shorter risetimes. The reason for this behavior is that the development of the discharge is slower than the voltage application, allowing the voltage across the laser gap to reach higher values before breaking takes

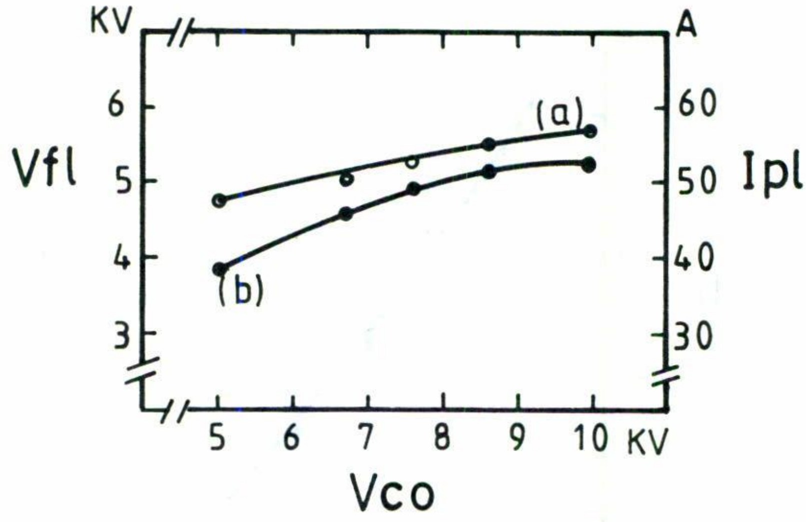

FIGURE 6. (a) Laser firing voltage V_{fl} and (b) peak current I_{pl} as functions of charging voltage V_{c0}.

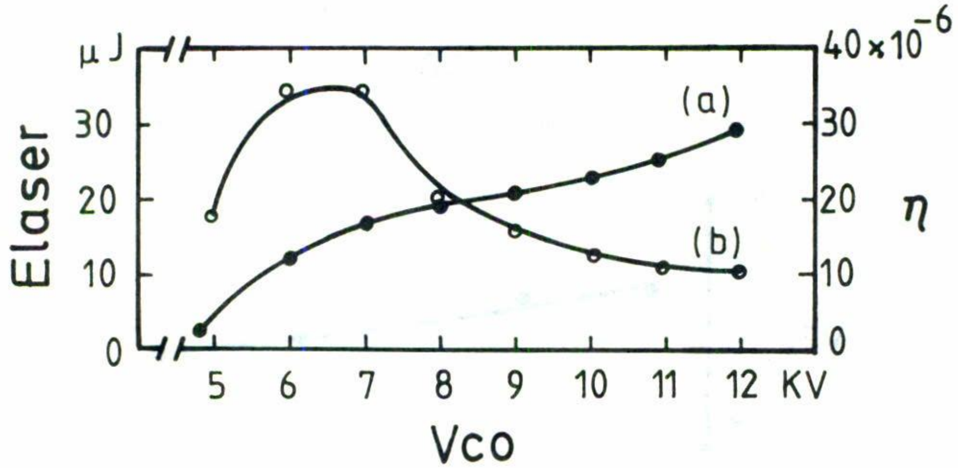

FIGURE 7. (a) Laser energy E_{laser} and (b) laser efficiency η as functions of charging voltage V_{c0}.

place. These results are in agreement with those obtained for the spark gap triggering process analyzed in Ref. [4].

In order to reach shorter risetimes, the inductance of the loop $SG + C_c + 2C_p$ should be reduced. Vázquez *et al.* [5] show that with a similar reduction in a Blumlein N_2 laser it is possible to improve the efficiency of the system rising the energy of the laser emission.

5. OTHER RESULTS

The laser operates at charging voltages ranging from 6 to 12 kV, pressures between 30 and 160 mbar providing 20 and more pulses per second. In Fig. 10 we show a plot of

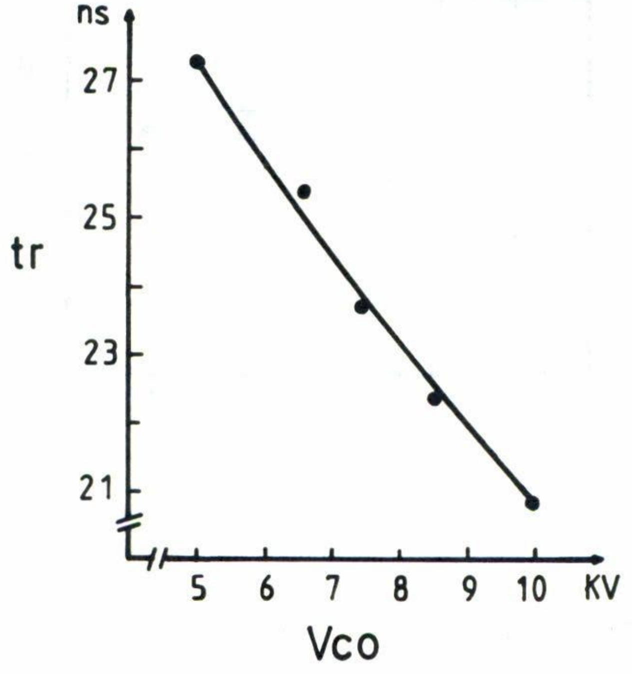

FIGURE 8. Voltage risetime t_r as a function of charging voltage V_{c0}.

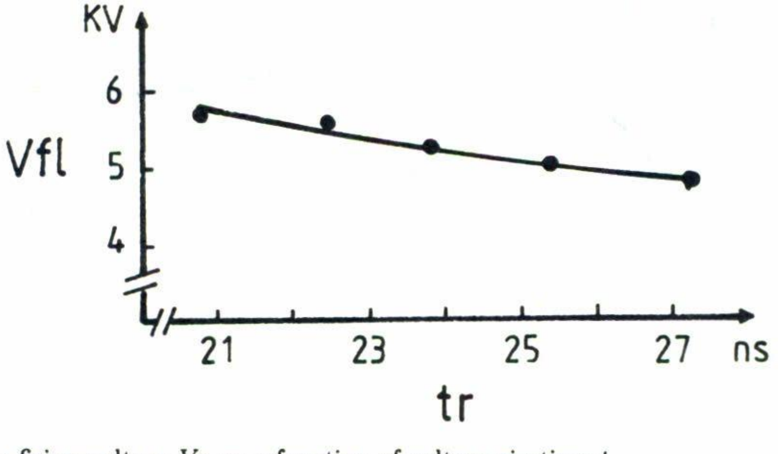

FIGURE 9. Laser firing voltage V_{fl} as a function of voltage risetime t_r.

the output laser energy as a function of the filling pressure for different voltages. The maximum observed energies were of about 40 μJ, the efficiency of the laser ranged between 0.15×10^{-4} and 0.35×10^{-4}.

6. CONCLUSIONS

A nitrogen laser based in a charge transfer circuit has been experimentally studied. Its

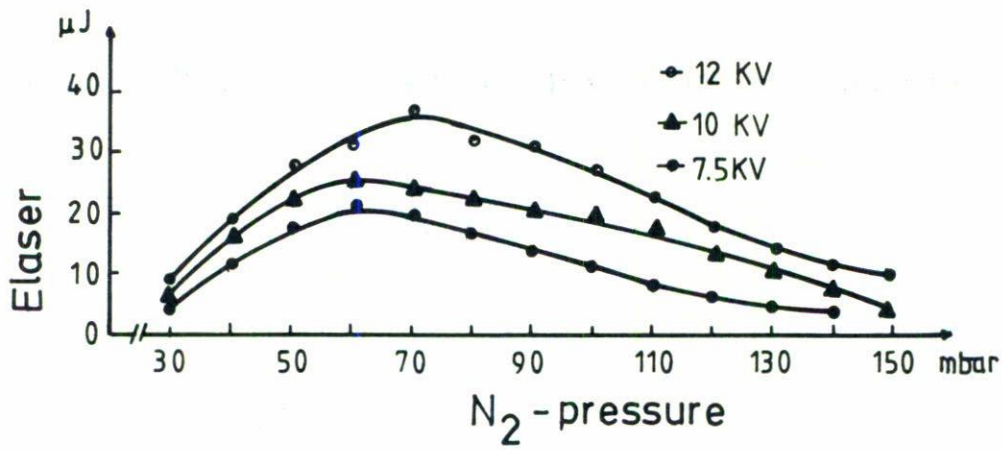

FIGURE 10. Output laser energy E_{laser} as a function of N_2 filling pressure for different charging voltages.

electrical behavior has been analyzed in great detail and also the characteristics of the laser emission. These studies provide a better understanding of the electrical behavior of the circuit, and show that current measurements are very important to determine the parameters of the circuit.

REFERENCES

1. A.D. Papadopoulus and A.A. Serafetinides, *J. Phys. D: Appl. Phys.* **24** (1991) 1917.
2. J. de la Rosa, W.H. Fonseca, P.A. Calva, R. Linares and A. Vázquez-Martínez, *Meas. Sci. Technol.* **5** (1994) 1109.
3. P. Persephonis, B. Giannetas, J. Parthenios, C. Gorgiades and A. Ioannou, *IEEE J. Quantum Electron.* **QE-29** (1993) 2371.
4. E. Kuffel and W. S. Zaengl, "High Voltage Engineering", Pergamon Press (1984), pp. 386-391.
5. A. Vázquez-Martínez and V. Aboites, *IEEE J. Quantum Electron. QE-29* (1993) 2364.